JOC The Journal of Organic Chemistry

Article

pubs.acs.org/joc

Thiol-Activated Triplet–Triplet Annihilation Upconversion: Study of the Different Quenching Effect of Electron Acceptor on the Singlet and Triplet Excited States of Bodipy

Caishun Zhang, Jianzhang Zhao,* Xiaoneng Cui, and Xueyan Wu

State Key Laboratory of Fine Chemicals, School of Chemical Engineering, Dalian University of Technology, E-208 West Campus, 2 Ling Gong Road, Dalian 116024, P.R. China

Supporting Information

ABSTRACT: Thiol-activated triplet–triplet annihilation (TTA) upconversion was studied with two different approaches, i.e., with 2,4-dinitrobenzenenesulfonyl (DNBS)-caged diiodoBodipy triplet photosensitizers (perylene as the triplet acceptor/emitter of the upconversion) and DNBS-caged Bodipy fluorophore as the triplet acceptor/emitter (PdTPTBP as the triplet photosensitizer, TPTBP = tetraphenyltetrabenzoporphyrin). The photophysical processes were studied with steady-state UV–vis absorption spectroscopy, fluorescence spectroscopy, electrochemical characterization, nanosecond transient absorption spectroscopy, and DFT/TDDFT computations. DNBS-caged triplet photosensitizer shows a shorter triplet state lifetime (24.7 μs) than the uncaged triplet photosensitizer (86.0 μs), and the quenching effect is due to photoinduced electron transfer (PET). TTA upconversion was enhanced upon cleavage of the DNBS moiety by thiols. On the other hand, the DNBS-caged Bodipy shows no fluorescence, but the uncaged fluorophore shows strong fluorescence; thus, TTA upconversion is able to be enhanced with the uncaged fluorophore as the triplet energy acceptor/emitter. The results indicate that the DNBS moiety exerts a significant quenching effect on the *singlet* excited state of Bodipy, but the quenching on the *triplet* excited state is much weaker. Calculation of the Gibbs free energy changes of the photoinduced electron transfer indicates that the singlet state gives a larger driving force for the PET process than the triplet state.

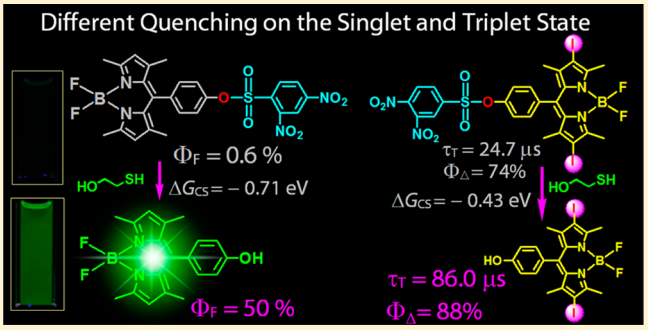

1. INTRODUCTION

Modulation of the excited states of chromophores is crucial for development of novel functional molecular materials, such as fluorescent molecular probes,[1−9] molecular switches,[10,11] and external stimuli-responsive molecular devices.[12−18] In this context, the methodologies of switching the *singlet* excited state have been well developed.[1] However, switching of the *triplet* excited states is rarely reported.[14,19−22] Switching of the triplet excited states will be very useful in the areas such as target activatable photodynamic therapy (PDT)[20,23−27] and molecular logic gates,[12] as well as for study of fundamental photochemistry of organic chromophores.[28]

Quenching of the triplet excited state may follow different principles as compared with that of quenching the singlet excited states, even with the same quencher. But this fundamentally important effect was rarely studied. For example, given that the quenching of the excited state is due to photoinduced electron transfer (PET), the Gibbs free energy changes (ΔG°_{CS}) of the PET processes for quenching of the singlet and triplet excited state will be different because the driving forces, the E_{00} values (the energy level of the excited state by which the PET is driven), are substantially *different* since the S_1 state and the T_1 state of typical fluorophores are substantially different; i.e., the S_1/T_1 state energy gap is usually large for polycyclic aromatic hydrocarbons. In this , the singlet excited state will offer a much *larger* driving force for the PET process than the triplet excited state of the same chromophore. However, investigations of such different quenching effects on the triplet and singlet excited states was not reported.

Concerning switching of the triplet excited state of organic chromophores, previously amino-azaBodipy was prepared as an acid-activatable PDT reagent.[20] The triplet state of the iodoazaBodipy chromophore was presumably quenched by PET from the appended N atom to the Bodipy chromophore. Protonation of the amino group will inhibit the PET; thus the triplet excited state yield is increased.[20] Fluorescence energy resonance transfer (FRET) was also used for switching of the triplet state of a Bodipy dyad.[12] In the presence of acid/base, one of the components in the dyad will be protonated so that the energy levels will be changed. As a result, a FRET process will be activated to compete with the intersystem crossing (ISC). On the other hand, photochromic chromophores, such as dithienylethene (DTE), were incorporated into the molecular structure of Ru(II) or Os(III) complexes to modulate the triplet excited states.[19] Recently, the singlet

Received: March 21, 2015
Published: May 5, 2015

DOI: 10.1021/acs.joc.5b00557
J. Org. Chem. 2015, 80, 5674−5686

Scheme 1. Preparation of the DNBS-Caged Triplet Photosensitizers C-1 and C-2 as Well as the DNBS-Caged Fluorophore Compound 2[a]

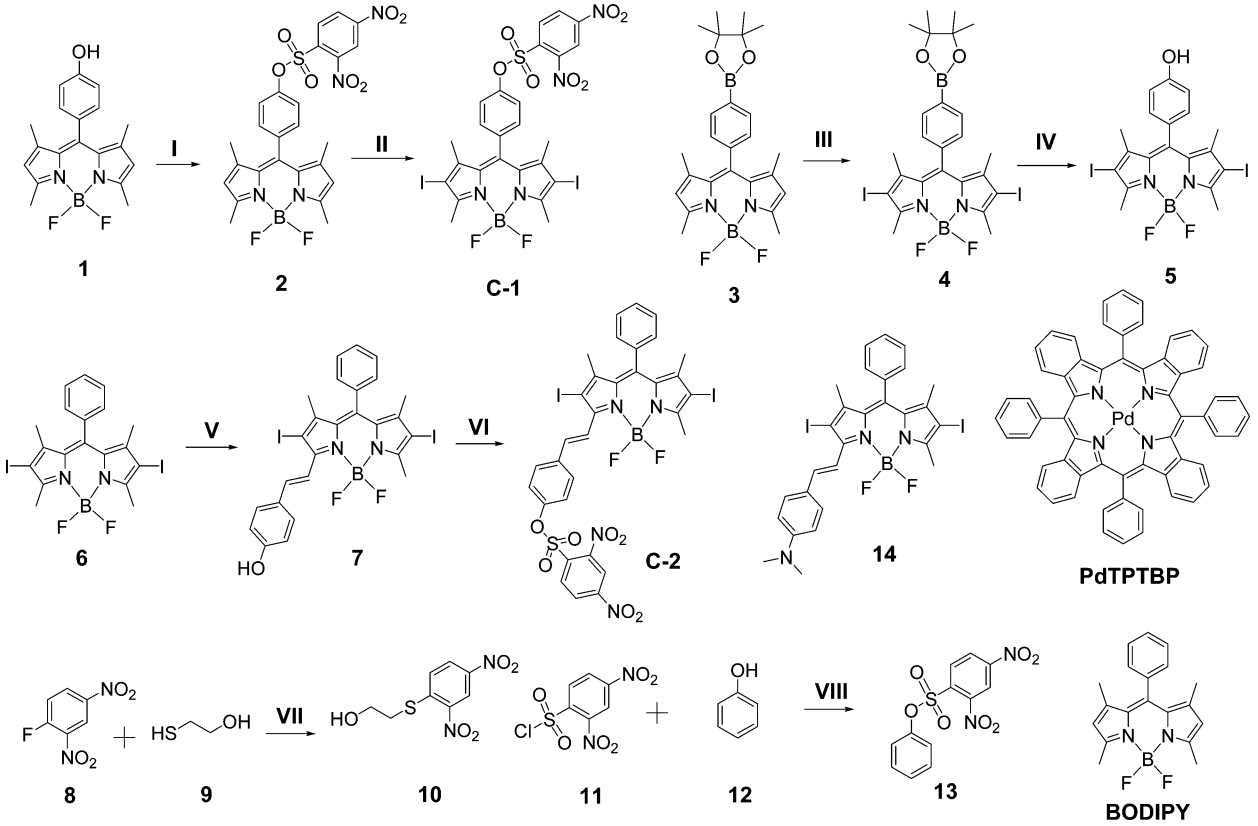

[a]Key: (I) dry CH_2Cl_2, TEA, 2,4-dinitrobenzenesulfonyl chloride, 50 °C, 10 h, yield 59.7%; (II) dry CH_2Cl_2, NIS, 5 h, 30 °C, yield 70%; (III) dry CH_2Cl_2, NIS, 5 h, 30 °C, yield 72.6%; (IV) H_2O_2, yield 43%; (V) dry toluene, piperidine, acetic acid and *p*-hydroxybenzaldehyde, 10 min, yield 12%; (VI) dry CH_2Cl_2, TEA, 2,4-dinitrobenzenesulfonyl, 50 °C, 10 h, yield 57%; (VII) dry $CHCl_3$ and TEA, yield 65%; (VIII) dry CH_2Cl_2 and TEA, 50 °C, 10 h, yield 54%.

Scheme 2. Cleavage Mechanism of the DNBS Moiety in C-1 by Thiols

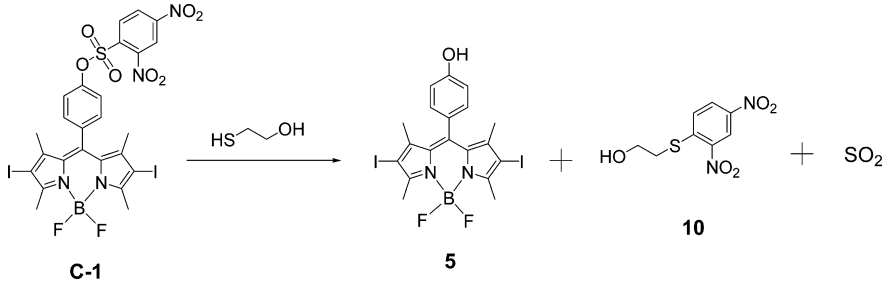

oxygen ($^1O_2$) production of Zn(II) porphyrin complex was switched by DTE via a photoswitchable intermolecular triplet energy transfer.[29] Previously, the 2,4-dinitrobenzenesulfonylamide (DNBS) moiety was used as an electron trap to switch the triplet excited state of the transition-metal complex to develop phosphorescent thiol probes or thiol-activatable PDT reagents.[30−32] For most of these studies, the switching of the triplet excited states was not studied in detail, for example, with the nanosecond transient absorption spectroscopy.[12,20]

Recently, we used DTE for preparation of a iodo-Bodipy-DTE triad, for which the triplet state manifold is able to be photoswitched (in aspects of both triplet-state lifetime and yield) by the photochromism of the DTE unit.[33] The switching effect was used for triplet−triplet annihilation (TTA) upconversion. We also used an intermolecular triplet−triplet energy transfer (TTET) approach for switching the TTA upconversion with DTE as the photo-responsive chromophore.[34] Controlling the singlet oxygen ($^1O_2$) photosensitizing of iodoBodipy with acid was reported.[35] In order to switch the visible light-absorption property, as well as the triplet-state property, we prepared rhodamine−C_{60} dyads for which the visible light absorption and the triplet state can be switched on by addition of acid.[36] However, much room is left to develop new methodologies for the triplet state switching, especially with chemical stimulation.

Herein, we report a new strategy for switching of the triplet-excited-state property of an organic chromophore and its application in controllable TTA upconversion, with chemical input. The approach is exemplified with thiol-cleavable DNBS-caged triplet photosensitizer (2,6-diiodoBodipy, Scheme 1).

DOI: 10.1021/acs.joc.5b00557
J. Org. Chem. 2015, 80, 5674−5686

Thiol compounds are important for keeping the intracellular redox homeostasis, and thiol compounds have been the targets for many molecular probes.[2] Herein, our method is based on the design of a "caged" triplet photosensitizer in which the triplet state was quenched by the PET from the diiodo-Bodipy chromophore to the intramolecular electron acceptor, DNBS (**C-1**, Scheme 1).[30−32] Previously, DNBS was used for controlling of the triplet excited state of metal complexes or bromoBodipy,[30−32] although the switching effect was not studied with nanosecond transient absorption spectroscopy. We envisage that this modulation can be conveyed to the triplet-state manifold of *organic* chromophore for switching of the TTA upconversion. The triplet-state lifetime of **C-1** will probably be shorter than that of the reference compound **5** (Scheme 1). The TTA upconversion will be less efficient with **C-1** as triplet photosensitizer because the critical step involved in TTA upconversion, the intermolecular triplet−triplet-energy-transfer (TTET), will be less efficient with the shorter triplet-state lifetime of the photosensitizer.[37,38] In the presence of thiols, the DNBS moiety will be cleaved off from **C-1** (Scheme 2); as a result, the triplet-state lifetime was extended as compared with that of **C-1**.[30] Correspondingly, the TTET will be enhanced.[38]

On the other hand, previously DNBS was used as an electron trap for design of fluorescent molecular probes for detection of thiols.[30,39−42] The fluorescence of this kind of molecular probes is usually quenched significantly with DNBS. In the presence of thiol analytes, such as cysteine, the DNBS moiety will be cleaved off from the fluorophore, and the fluorescence will be enhanced.[39,43,44] Inspired by these studies, herein we also studied a complementary approach for switching of TTA upconversion, that is, to switch the emissive singlet excited state of Bodipy chromophore (compound **2**, Scheme 1). Compound **2** was used as triplet acceptor/emitter of TTA upconversion, with Pd(II) tetraphenyltetrabenzoporphyrin (TPTBP) as triplet photosensitizer. The results show that DNBS is *more effective* for quenching of the singlet excited state of Bodipy than quenching of the triplet excited state of the same Bodipy chromophore.

The photophysical properties of the compounds were studied with steady-state UV−vis absorption and fluorescence emission spectra, nanosecond transient absorption spectroscopy, electrochemical characterization (cyclic voltammetry), and DFT/TDDFT computations. We demonstrated that the switching of the triplet state and singlet excited state with the thiol-cleavable cage moiety can be used for switching of the TTA upconversion. This information is useful for designing new switchable triplet photosensitizers and for application of these compounds in activatable PDT and chemical stimuli-controlled TTA upconversion.

2. RESULTS AND DISCUSSION

2.1. Molecular Designing Rationales. Previously, it was shown that the DNBS moiety is a strong electron acceptor for quenching of fluorescence.[41,43] This property was used in the design of thiol-selective fluorescent molecular probes. With DFT calculations, we show that the S_1 state of the chromophore was modulated with the attachment and the cleavage of the DNBS moiety.[40−42] The S_1 state of the caged fluorophore is a dark state, whereas the uncaged fluorophore gives the S_1 state as emissive state.[40−42] However, the quenching effect of DNBS on the singlet excited state and triplet excited state of the same chromophore was not compared.

Herein, we designed compound **C-1** (Scheme 1), in which the Bodipy moiety was iodinated at the 2,6-position for triplet formation. Bodipy was selected as the chromophore, due to its satisfactory photophysical properties.[45−50] We envisaged that the triplet excited state of 2,6-diiodoBodipy may be quenched by the DNBS moiety (in both aspects of lifetime and yield), whereas cleavage of the DNBS moiety may lead to the recovery of the triplet excited state of the 2,6-diiodoBodipy. In order to study the mechanism of the triplet state switching, we prepared **C-2** (Scheme 1), in which the styryl diiodo-Bodipy shows a much lower triplet-state energy level than the 2,6-diiodoBodipy unit in **C-1**. The preparation of the compounds is based on routine synthetic methods. The compounds were obtained in moderate to satisfactory yields.

As a complementary study, we investigated the quenching effect of DNBS moiety on the singlet excited state of Bodipy, i.e., the fluorescence, with compounds **1** and **2** (Scheme 1). The fluorescence emissions of **1** and **2** were compared. The quenching effect of DNBS on the singlet excited state of Bodipy (fluorescence) is more significant than that on the triplet excited state. Quenching of the singlet excited state of Bodipy was also used for switching of TTA upconversion.

2.2. UV−vis Absorption and Fluorescence Emission Spectroscopies. First, the UV−vis absorption of the compounds was studied (Figure 1). The dyad **C-1** and the reference compounds **5** and **6** show similar UV−vis absorption spectra. This result indicates that there is no significant electronic interaction between the chromophores in **C-1** at the ground state.[41] For **C-2**, however, a different UV−vis absorption spectrum was observed as compared to the reference compound **7**. This result is reasonable since the DNBS moiety is directly attached on the π-conjugation framework in **C-2**, which is different from the molecular structural profile of **C-1**.

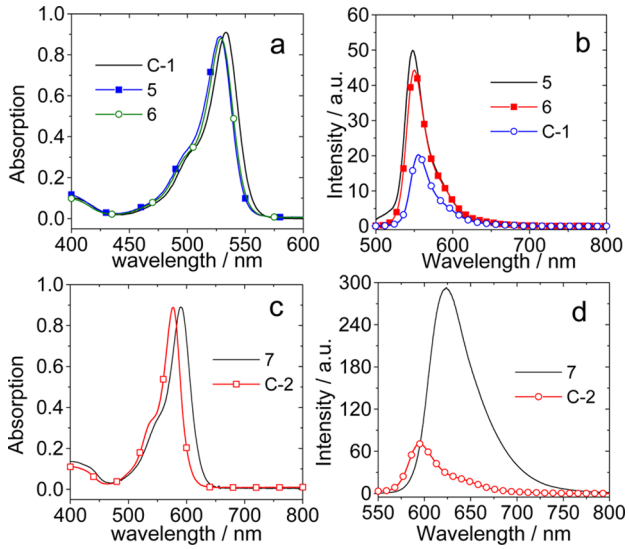

Figure 1. (a) UV−vis absorption spectra of **C-1**, **5**, and **6**. (b) Fluorescence emission spectra of **C-1**, **5**, and **6** (λ_{ex} = 480 nm; optically matched solution was used). (c) UV−vis absorption spectra of **7** and **C-2**. (d) Fluorescence emission spectra of **7** and **C-2** (λ_{ex} = 530 nm; optically matched solutions were used). For the absorption spectra, $c = 1.0 \times 10^{-5}$ M in CH_3CN, 20 °C.

DOI: 10.1021/acs.joc.5b00557
J. Org. Chem. 2015, 80, 5674−5686

The fluorescence of the compounds was studied (Figure 1b,d). Reference compounds **5** and **6** show similar emission properties (note that optically matched solutions were used in the comparison of the fluorescence of the compounds). For **C-1**, however, much weaker fluorescence was observed as compared with that of compounds **5** and **6**. This result indicates that the fluorescence of the diiodo-Bodipy part in **C-1** was quenched, most likely by the PET process.[40,41] Similar results were found for **C-2** and the reference compound **7** (Figure 1d). The fluorescence emission of **C-2** is much weaker than the reference compound **7**. It should be noted that the switching effect of the DNBS moiety on the fluorescence of the uniodinated Bodipy compounds is more significant.[40−42] Generally, the singlet-excited-state lifetimes of **C-1** and **C-2** are much shorter than those of the uniodinated compounds; thus, it is more difficult for the electron transfer to compete with the fast radiative decay of the singlet excited state of **C-1** and **C-2**.[51]

The UV−vis absorption and the fluorescence emission spectral changes of **C-1** and **C-2** in the presence of thiol compound (2-mercaptoethanol) were studied (Figure 2). For **C-1**, the UV−vis absorption spectrum did not show significant change upon addition of thiol.[40−42] For **C-2**, however, the absorbance decreased upon addition of 2-mercaptoethanol. Fluorescence enhancement was observed for both **C-1** and **C-2** in the presence of 2-mercaptoethanol (Figure 2c and 2d). This result is in agreement with the previously studied fluorescent thiol molecular probes.[40−42]

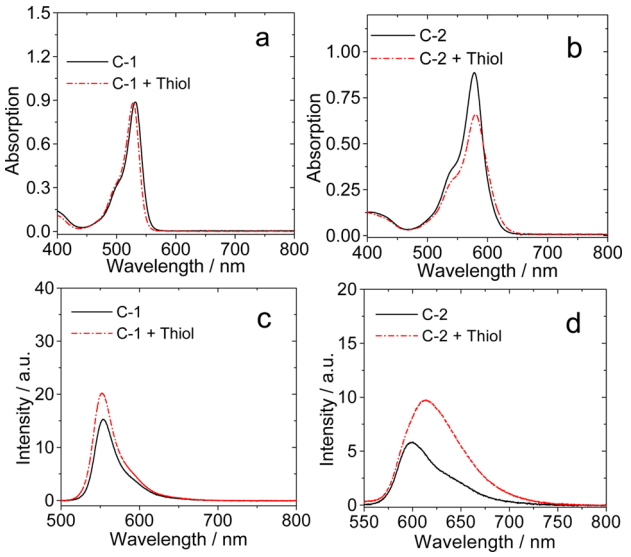

Figure 2. UV−vis absorption spectra of (a) **C-1** and (b) **C-2** before and after addition of thiol. Fluorescence emission of (c) **C-1** (λ_{ex} = 470 nm) and (d) **C-2** (λ_{ex} = 530 nm) before and after addition of thiol (optically matched solutions were used). For UV−vis absorption spectra, c = 1.0 × 10^{-5} M. For fluorescence emission, c[**C-1** or **C-2**]:c[thiol] = 1:200, and the thiol used in the study is mercaptoethanol. In CH_3CN, 20 °C.

The UV−vis absorption and fluorescence properties of compounds **1** and **2** were also studied (Figure 3). The two compounds show similar absorption, with maximum absorptions at 503 and 506 nm for **1** and **2**, respectively (Figure 3a). The two compounds show drastically different fluorescence properties (Figure 3b); compared to compound **1**, the fluorescence of compound **2** was completely quenched. The fluorescence of compound **1** was compared with the unsubstituted Bodipy (Figure 3c, with optically matched solution). Compound **1** gives lower fluorescence emission (Φ_F = 50%) than unsubstituted Bodipy (Φ_F = 90%).

The photophysical properties of the compounds were summarized in Table 1. The fluorescence quantum yields of

Table 1. Photophysical Parameters of the Compounds[a]

	λ_{abs}	ε[c]	λ_{em}	Φ_F[d] (%)	τ_F[e] (ns)	τ_T[f] (μs)	Φ_T[h] (%)
1[b]	503	9.04	515	50.0	4.28		
2[b]	506	9.26	519	0.6	1.67		
5	529	8.92	547	4.1	0.18	171.3	92.5
7	590	8.91	624	23.6	1.53	4.4	64.7
C-1	533	9.10	556	1.7	0.10	24.7	88.6
C-1[g]	528	8.86	550	1.9	0.15	86.0	
C-2	576	8.88	594	3.4	0.37	2.7	57.6
C-2[g]	580	6.60	596	8.9	0.50	3.1	

[a]In CH_3CN (1.0 × 10^{-5} M). [b]In toluene. [c]Molar absorption coefficient. ε: 10^4 M^{-1} cm^{-1}. [d]Fluorescence quantum yields. Bodipy (Φ_F = 90.0% in toluene) was used as standard for **1** and **2**. **6** (Φ_F = 2.7% in CH_3CN) was used as standard for **5**, **C-1**, and **C-1** after cleavage of the DNBS moiety by thiols. **14** (Φ_F = 9.5% in toluene) was used as standard for **7**, **C-2**, and **C-2** after cleavage of the DNBS moiety by thiols. [e]Fluorescence lifetimes. [f]Triplet state lifetimes, measured by transient absorptions. [g]After cleavage of the DNBS moiety by thiols. [h]Triplet state quantum yield, with Rose Bengal as stand (Φ_T = 0.9 in methanol).

C−1, **C-2**, and the cleavaged products are low, which is due to the iodination of the Bodipy chromophores.[52−54] It is noted that the fluorescence lifetimes of **C-1**, **C-2** and the cleavage product are short, which are due to the influence of the DNBS electron acceptor (PET) and the iodination of the Bodipy chromophore (ISC effect).[20,55] These results are drastically

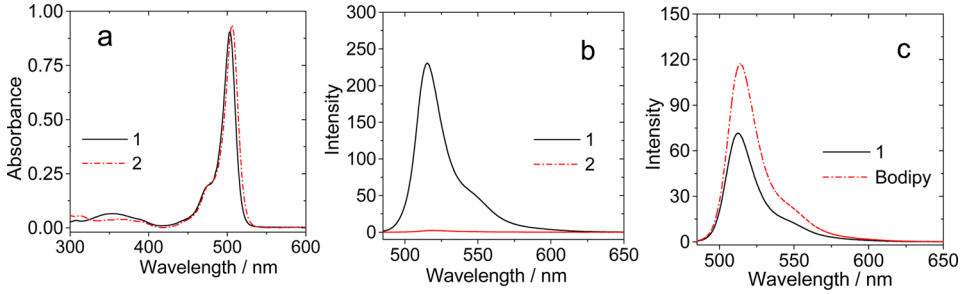

Figure 3. (a) UV−vis absorption spectra of compounds **1** and **2**, c = 1.0 × 10^{-5} M. (b) Fluorescence emission of compound **1** and **2** (λ_{ex} = 470 nm; optically matched solutions were used). (c) Fluorescence emission of **1** and Bodipy. λ_{ex} = 470 nm. Optically matched solutions were used. In toluene, 20 °C.

DOI: 10.1021/acs.joc.5b00557
J. Org. Chem. 2015, 80, 5674−5686

different from the previously reported Bodipy-DNBS based fluorescent thiol probes; those probes show a fluorescence-switching effect.[52−54]

$$k_{ET} = \left[\frac{\Phi_{ref}}{\Phi_{sen}} - 1\right]/\tau_{ref} \quad (1)$$

The photoinduced intramolecular electron transfer rate constants in the caged fluorophore and the triplet photosensitizers were calculated with eq 1,[56] when k_{ET} is the electron transfer rate constant, Φ_{ref} and τ_{ref} is the fluorescence quantum yield and the lifetime of the reference compounds (**5** or **7**), and Φ_{Sen} is the fluorescence lifetime of the corresponding caged photosensitizers (**C-1** or **C-2**) (Table 2). It was found the PET process in compound **2** is faster than that in **C-1** and **C-2**. This result can be used to rationalize the fully quenched fluorescence in **C-1**.

Table 2. Rate Constants for Singlet Energy Transfer[a]

	Φ_{PL}(ref)/Φ_{PL}(sen)[c]	k_{ET}[d] (s^{-1})	τ_F[e] (ns)
C-1	2.4	7.83×10^9	0.18[f]
C-2	6.9	3.88×10^9	1.53[g]
2[b]	83.3	2.13×10^{10}	3.87[h]

[a]In acetonitrile. [b]In toluene. [c]Ratio of the fluorescence quantum yields of the reference compounds (**5** and **7**) and the corresponding DNBS caged photosensitizers (**C-1** and **C-2**). [d]Photoinduced intramolecular electron transfer rate constants. [e]Fluorescence lifetime. [f]Fluorescence lifetime for compound **5**. [g]Fluorescence lifetime for compound **7**. [h]Fluorescence lifetime for compound **1**.

2.3. Nanosecond Transient Absorption Spectroscopy.

In order to study the switching of the triplet excited state of the compounds upon caging with DNBS and cleavage of the DNBS moiety by thiols, the nanosecond transient absorption spectroscopy of the compounds **C-1** and **C-2** in the absence and in the presence of thiols was studied. First, nonpolar solvent toluene was used for study of the triplet state of **C-1** (Figure 4). The TA spectra of **C-1** in toluene were recorded (Figure 4a). The bleaching band at 538 nm was observed upon pulsed laser excitation, which is due to the depletion of the ground state of the diiodoBodipy moiety upon photoexcitation. Excited-state absorptions (ESA) in the region of 380−480 and 584−774 nm were observed, which are attributed to the absorption of the triplet state of 2,6-diiodoBodipy moiety (spin-allowed $T_1 \rightarrow T_n$ transitions).[52,57] In toluene, the triplet-state lifetime of **C-1** was determined as 187.7 μs (Figure 4b). In the presence of thiol, the TA spectra hardly give any changes (Figure 4c). The triplet-state lifetime was determined as 189.9 μs (Figure 4d), very close to that of the caged triplet photosensitizer (**C-1**). The singlet oxygen ($^1O_2$) quantum yields (Φ_Δ) of **C-1** and the cleaved product were determined as 0.59 and 0.65, respectively (Table S1, Supporting Information). Thus, we conclude that there is no significant switching effect upon addition of thiol for **C-1** in toluene. It was well-known that the PET of multichromophore compounds is unlikely to occur in nonpolar solvents such as toluene;[58−60] thus, we postulate that the there is no significant intramolecular PET for **C-1** in toluene.

Similar results were observed in polar solvents such as dichloromethane (DCM); the triplet-state lifetimes of **C-1** before and after cleavage with thiol are 166.6 and 168.1 μs, respectively (Supporting Information, Figure S22). Note that the triplet-state lifetimes of **5** in DCM and toluene is 151.4 and

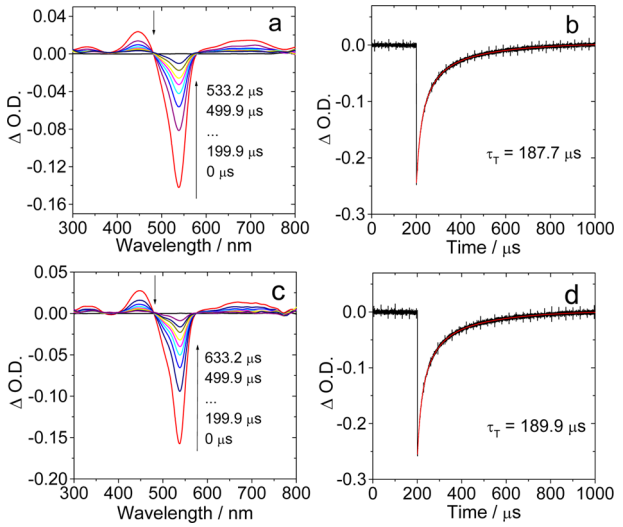

Figure 4. (a) Nanosecond transient absorption spectra of **C-1** and (b) the corresponding decay trace at 533 nm. (c) Nanosecond transient absorption spectra of **C-1** upon addition of mercaptoethanol and (d) the corresponding decay trace at 533 nm (λ_{ex} = 529 nm). c[**C-1**]:c[mercaptoethanol] = 1:200. After addition of the thiols, the solution was allowed to stand for 30 min before measurement of the spectra. c[**C-1**] = 1.0×10^{-5} M in toluene, 20 °C.

183.4 μs, respectively (Supporting Information, Figure S23), which indicated that the different triplet lifetime of **C-1** in toluene and DCM is due to the diiodo-Bodipy moiety, not any PET process between the diiodo-Bodipy and DNBS moiety.

The TA spectra of **C-1** in polar solvent, such as acetonitrile, were studied (Figure 5). Although the bleaching and the transient positive absorption profiles of **C-1** in the absence and in the presence of thiols are similar (Figure 5a, c), the triplet state lifetime show substantial difference (Figure 5b and 5d). The triplet state lifetime of **C-1** in acetonitrile was determined

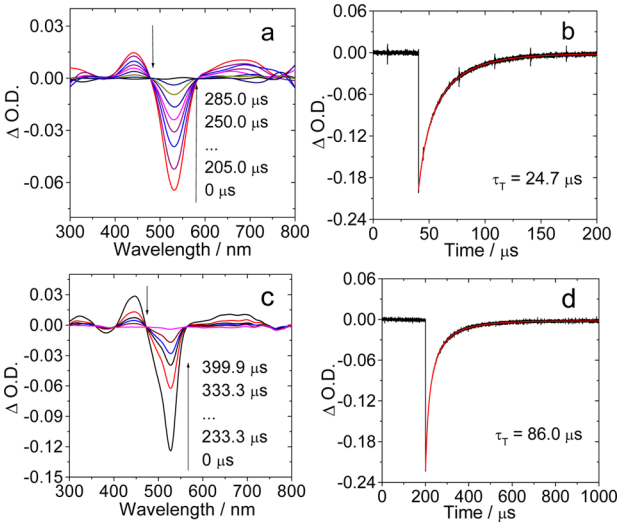

Figure 5. Nanosecond transient absorption of (a) **C-1** and (b) the decay trace at 533 nm. Nanosecond transient absorption of (c) **C-1** after cleavage of the DNBS moiety by mercaptoethanol and (d) the decay trace at 533 nm. In all cases, c[**C-1**]:c[thiol] = 1:200m λ_{ex} = 529 nm. In CH_3CN. After addition of mercaptoethanol, the solution was allowed to stand for 30 min before measurement of the spectra. c[photosensitizers] = 1.0×10^{-5} M, 20 °C.

DOI: 10.1021/acs.joc.5b00557
J. Org. Chem. 2015, 80, 5674−5686

as 24.7 μs, but the lifetime was significantly extended to 86.0 μs in the presence of thiols, i.e. cleavage of the DNBS moiety. Thus, we propose that the PET in **C-1** is significant in polar solvent such as acetonitrile. This is a known fact for intramolecular PET in multichromophore compounds.[58−60] The Φ_Δ value of **C-1** changed from 0.74 to 0.88 upon cleavage with thiol in CH_3CN (Table S1, Supporting Information). Thus, switching of the triplet excited state of **C-1** is implemented with thiol as an external chemical input. Previously, we studied a thiol-selective phosphorescent molecular probe in which the DNBS moiety is an electron acceptor and the Ru(II) complex is the phosphorescent chromophore.[30] In order to reveal the different triplet-state lifetimes of **5** and **C-1** after cleavage of the DNBS moiety by thiols, Stern−Volmer quenching plots of **5** in the presence of compounds **10** and **13** (quenchers) were studied. Both compounds **10** and **13** have a strong quenching effect on the triplet state lifetime of **5** (see the Supporting Information, Figure S33−S35).

Similar studies were carried out for **C-2** (Figure 6). Interestingly, no substantial triplet-state lifetime changes were

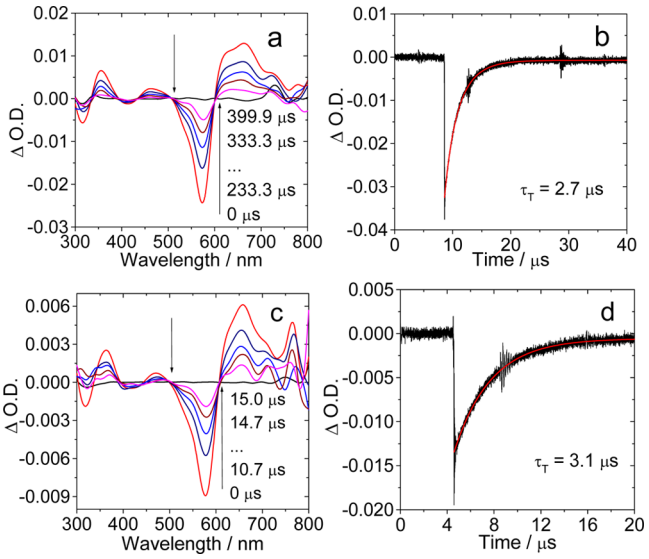

Figure 6. Nanosecond transient absorption of (a) **C-2** and (c) after cleavage of the DNBS moiety by mercaptoethanol. Decay traces of (b) **C-2** and (d) after cleavage of the DNBS moiety by thiols at 586 n, (c[**C-2**]:c[thiol] = 1:200) excited with nanosecond pulsed laser (λ_{ex} = 589 nm). After addition of the thiols, the solution was allowed to for 30 min before measurement of the spectra. c[photosensitizers] = 1.0 × 10^{-5} M. In CH_3CN, 20 °C.

observed for **C-2** in the presence of thiol, even in polar solvents such as acetonitrile. For example, the triplet-state lifetime of **C-2** is 2.7 μs in acetonitrile in the absence of thiol. In the presence of thiol, the triplet-state lifetime was only slightly extended to 3.1 μs. Similar triplet state lifetimes were also observed for **C-2** in toluene and dichloromethane (Supporting Information, Figures S24 and S25). The cleaved chromophore, i.e., compound **7**, shows a similar triplet-excited-state lifetime (Supporting Information, Figure S26). In CH_3CN, the Φ_Δ was determined as 0.20 for **C-2** as well as for the cleaved product (Table S1).

Compounds **1** and **2** are devoid of any heavy atoms; thus, no significant triplet-state formation was observed with the compounds. Instead, as triplet-state acceptor for the TTA upconversion, quenching of the triplet state of PdTPTBP with compounds **1** and **2** was studied (Figure 7). With compound **2**,

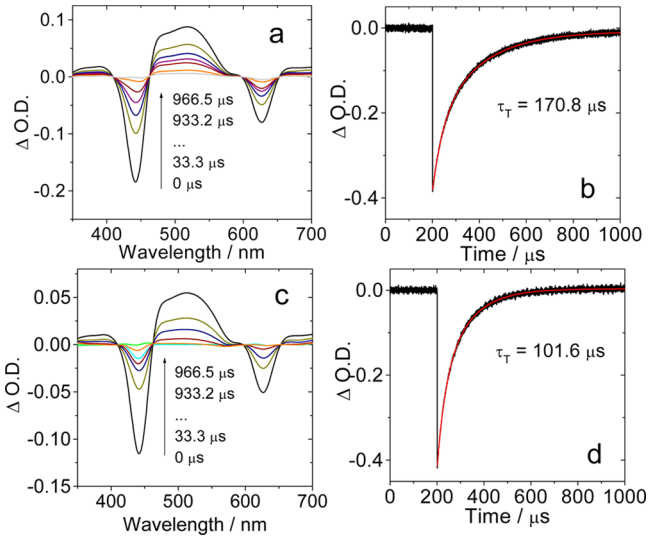

Figure 7. Nanosecond transient absorption of (a) PdTPTBP and (b) the corresponding decay trace at 440 nm. (c) Nanosecond transient absorption of PdTPTBP in the presence of compound **2** and (d) the decay trace at 440 nm. c[PdTPTBP] = 5.0 × 10^{-6} M. c[compound **2**] = 2.0 × 10^{-6} M in toluene. λ_{ex} = 445 nm, 20 °C.

substantial quenching effect on the triplet state of PdTPTBP was observed (Figure 7c,d). For example, nanosecond transient absorption spectra of PdTPTBP upon pulsed laser excitation show two bleaching bands at 442 and 627 nm. These bleaching bands are due to the depletion of the ground state of PdTPTBP. The inherent triplet state lifetime of PdTPTBP was determined as 170.8 μs (Figure 7b). In the presence of compound **2** (2.0 × 10^{-6} M. 1:0.4 molar ratio for PdTPTBP/compound **2**), the triplet-state lifetime was reduced to 101.6 μs (for detail Stern−Volmer quenching plots, see Figure 12 and the Supporting Information, Figures S38 and S39).

Interestingly, no bleaching band of the Bodipy moiety of compound **2** (at ca. 500 nm) was observed; this result indicates that the Bodipy moiety in compound **2** is not the ultimate triplet energy trap. We postulate the quenching of the triplet excited state of PdTPTBP by the DNBS moiety is due to intermolecular electron transfer.[61]

2.4. Electrochemical Studies: Free Energy Changes of the Photoinduced Electron Transfer. The electrochemical properties of the complexes were studied by cyclic voltammetry (Figure 8). For the reference compound **5**, a reversible oxidation wave was observed at +0.94 V and a reversible reduction wave was observed at −1.26 V. For reference compounds **10** and **13**, irreversible reduction peaks at −1.31 and −0.95 V were observed. The reversible oxidation wave at +0.97 V of **C-1** is attributed to the 2,6-diiodoBodipy moiety (electron donor). The irreversible oxidation wave of **C-1** at −0.93 V can be attributed to the electron-acceptor moiety (Table 3). For reference compound **7**, a reversible oxidation wave was observed in which the half-wave potential is +0.68 V, and a reversible reduction wave can also be observed which half-wave potential is −1.15 V. Due to the poor solubility of **C-2**, no signal can be observed.

DOI: 10.1021/acs.joc.5b00557
J. Org. Chem. 2015, 80, 5674−5686

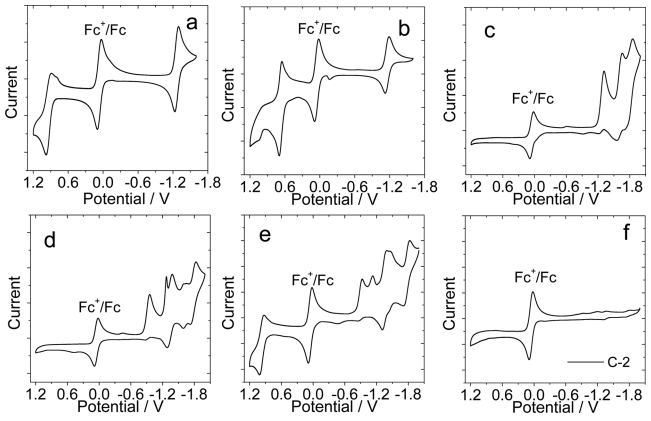

Figure 8. Cyclic voltammogram of the dyad photosensitizers **5**, **7**, **10**, **13**, **C-1**, and **C-2**. Ferrocene (Fc) was used as internal reference: (a) compound **5**, (b) compound **7**, (c) compound **10**, (d) compound **13**, (e) compound **C-1**, (f) compound **C-2**. Due to poor solubility, no satisfactory signal was observed for **C-2**. In deaerated CH_3CN solutions containing 5.0×10^{-4} M photosensitizers, 0.10 M Bu_4NPF_6 as supporting electrode, $Ag/AgNO_3$ reference electrode. Scan rates: 0.1 V/s, 20 °C.

Table 3. Redox Potentials of Bodipy Photosensitizers for Study of the Potential Intramolecular Electron transfer. Anodic and Cathodic Peak Potential[a]

	$E_{1/2}$(ox) (V)	$E_{1/2}$(red) (V)
1	0.82	−1.53
2	0.87	−0.88
5	0.94	−1.26
7	0.68	−1.15
10	*b*	−1.31
13	*b*	−0.95
C-1	0.97	−0.93
C-2	*b*	*b*

[a]In deaerated CH_3CN solutions containing 5.0×10^{-4} M photosensitizers, 0.10 M $Bu_4N[PF_6]$ as supporting electrode, $Ag/AgNO_3$ reference electrode. Scan rates: 0.1 V/s, 20 °C. [b]Not observed.

The free energy changes of the intramolecular electron transfer process can be calculated with the Rehm−Weller equation (eqs 2 and 3)[59]

$$\Delta G^{\circ}_{CS} = e[E_{OX} - E_{RED}] - E_{00} + \Delta G_S \quad (2)$$

$$\Delta G_S = -\frac{e^2}{4\pi\varepsilon_S\varepsilon_0 R_{CC}} - \frac{e^2}{8\pi\varepsilon_0}\left(\frac{1}{R_D} + \frac{1}{R_A}\right)\left(\frac{1}{\varepsilon_{REF}} - \frac{1}{\varepsilon_S}\right) \quad (3)$$

where ΔG_S is the static Coulombic energy which is described by eq 3, e = electronic charge, E_{OX} = half-wave potential for one-electron oxidation of the electron-donor unit, E_{RED} = half-wave potential for one-electron reduction of the electron-acceptor unit, $E_{0,0}$ = energy level approximated with the intersection of fluorescence emission and UV−vis absorption after normalization (for the singlet excited state), ε_S = static dielectric constant of the solvent, R_{CC} = center-to-center separation distance between the electron donor (diiodoBodipy) and electron acceptor (DNBS), determined by DFT optimization of the geometry, R_{CC} (**C-1**) = 8.6 Å, R_{CC} (**C-2**) = 13.8 Å, R_D is the radius of the electron donor, R_D (**C-1**) = 4.3 Å, R_D (**C-2**) = 8.4 Å. R_A is the radius of the electron acceptor, R_A (**C-1**) = 4.9 Å, R_A (**C-2**) = 4.9 Å. ε_{REF} is the static dielectric constant of the solvent used for the electrochemical studies, and ε_0 is permittivity of free space. The solvents used in the calculation of Gibbs free energy of the electron transfer are toluene (ε_S = 2.4), CH_2Cl_2 (ε_S = 9.1) and acetonitrile (ε_S = 37.5).

Energy levels of the charge-separated states (E_{CS}) and charge recombination energy state (ΔG_{CR}) can be calculated with eqs 4 and 5.[2] The data were collected in Table 4.

$$E_{CS} = e[E_{OX} - E_{RED}] + \Delta G_S \quad (4)$$

$$\Delta G_{CR} = -(\Delta G_{CS} + E_{00}) \quad (5)$$

The Gibbs free energy changes of the electron transfer in **C-1** and **C-2** indicate that electron transfer is inefficient in nonpolar solvent, such as toluene. This conclusion derived from the electrochemical data is in agreement with the nanosecond transient absorption spectra of **C-1** (Figure 4 and 5). The driving force for PET in medium-polarity solvent is also small. The driving force is large in polar solvents such as acetonitrile (Table 4). The Gibbs free energy changes of the PET process of **C-1** were calculated as −0.43 eV in acetonitrile. In less polar solvents, smaller driving force for PET was observed (Table 4). A similar trend was observed for **C-2**. It should be noted that the triplet-state property of **C-1**, such as the lifetime, was not affected by PET, unless the energy level of the charge-transfer-state (CST) is lower in energy level than that of the triplet excited state (see later section).

In order to reveal the mechanism of the quenching of fluorescence with DNBS moiety in compound **2**, the electrochemical data of compounds **1** and **2** were also recorded (Figure 9). Following methods similar to those of compounds **C-1** and **C-2**, the Gibbs free energy changes for the PET process in compound **2** were calculated, and the data are listed in Table 4. The results show that for compound **2** the driving force for the PET process always exists, even for nonpolar solvents such as toluene, and in comparison, the driving force for the PET in other solvents is larger than that of compounds

Table 4. Free Energy Changes of Charge Separation (ΔG_{CS}), Free Energy Changes of Charge Recombination (ΔG_{CR}) and Energy Levels of Charge Separation Energy States (E_{CS}) of Compounds 2, C-1, and C-2

	$\Delta G_{CS}{}^a$ (eV)	$\Delta G_{CS}{}^a$ (eV)	$E_{CS}{}^a$ (eV)	$\Delta G_{CS}{}^b$ (eV)	$\Delta G_{CS}{}^b$ (eV)	$E_{CS}{}^b$ (eV)	$\Delta G_{CS}{}^c$ (eV)	$\Delta G_{CS}{}^c$ (eV)	$E_{CS}{}^c$ (eV)
2	−0.27,[d] +0.63[e]	−1.52	+1.52	−0.61,[d] +0.29[e]	−1.17	+1.17	−0.71,[d] +0.19[e]	−1.71	+1.71
C-1	+0.14,[d] +0.90[e]	−2.42	+2.42	−0.30,[d] +0.46[e]	−1.98	+1.98	−0.43,[d] +0.33[e]	−1.85	+1.85
C-2	−0.02,[d] +0.79[e]	−2.10	+2.10	−0.40,[d] +0.40[e]	−1.71	+1.71	−0.51,[d] +0.30[e]	−1.61	+1.61

[a]In toluene. [b]In CH_2Cl_2. [c]In acetonitrile. [d]$E_{0,0}$ = energy level approximated with the intersection of fluorescence emission and UV−vis absorption after Normalization at the singlet excited state. [e]$E_{0,0}$ = energy level approximated with the triplet state energy level by DFT calculation. All of the calculations (except **C-2**) are based on the first oxidation reduction potential. For **C-2**, the calculation is base on the first oxidation reduction potential of compound **7** and **13**.

DOI: 10.1021/acs.joc.5b00557
J. Org. Chem. 2015, 80, 5674−5686

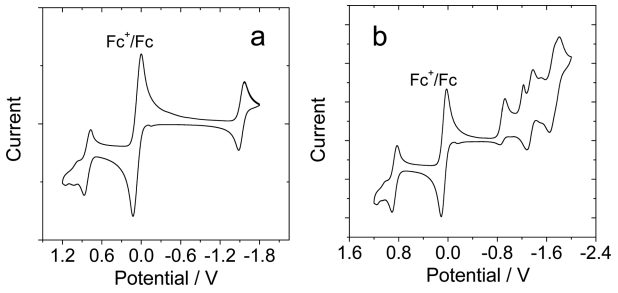

Figure 9. Cyclic voltammogram of photosensitizers (a) **1** and (b) **2**. Ferrocene (Fc) was used as internal reference. In deaerated CH_3CN solutions containing 5.0×10^{-4} M photosensitizers with the ferrocene, 0.10 M Bu_4NPF_6 as supporting electrode, $Ag/AgNO_3$ reference electrode, Scan rates: 0.1 V/s, 20 °C.

C-1 and **C-2**. Thus, we postulate that quenching of the singlet excited state of Bodipy by DNBS moiety is more efficient than quenching of the triplet excited state of Bodipy. The reason for this different quenching behavior is the different energy level of the singlet and triplet excited state of Bodipy moiety. These results indicate that designing triplet photosensitizers which show higher triplet state energy level is beneficial for switching/activation with external stimulus.

2.5. DFT Calculations: Rationalization of the Photophysical Properties. DFT calculations were carried out for rationalization of the photophysical properties of the compounds.[62−65] First, the spin density surfaces of **C-1** and **C-2** were calculated (see the Supporting Information, Figure S43).[66,67] The T_1 triplet excited states of both **C-1** and **C-2** are confined on the diiodo-Bodipy moieties, which are in agreement with the nanosecond transient absorption spectra of the compounds. For **2**, the spin density surface is confined on the Bodipy moiety, not the DNBS moiety. Thus, the T_1 state of compound **2** is localized on the Bodipy part, not DNBS the part.

In order to study the photophysical processes such as the electron transfer, the ground-state geometries of the compounds were optimized, and the UV−vis absorption and the virtual $S_0 \rightarrow T_n$ excitations of the triplet photosensitizers were calculated on the basis of the optimized ground-state geometry with the TDDFT method (see the Supporting Information, Figure S44 and Table S2). The energy-minimized geometry of **C-1** and **C-2** at the ground state indicated that the electron withdrawing group (2,4-dinitrobenzene part) keeps away from the electron-donating group (2,6-diiodoBodipy part). For **C-1**, the phenyl moiety connected to the Bodipy core takes a perpendicular geometry against the π-core of the 2,6-diiodoBodipy moiety. For **C-2**, the styryl moiety is almost coplanar with Bodipy π-core; thus, large π-conjugation resulted.

The calculated UV−vis absorption bands for **C-1** ($S_0 \rightarrow S_1$ and $S_0 \rightarrow S_1$) are located at 575 and 468 nm and HOMO → LUMO and HOMO → LUMO+1 are the respective major components of the transitions. For both processes, the electron density transferred from the electron-donating group (2,6-diiodoBodipy part) to the electron-withdrawing part (2,4-dinitrobenzenesulfunyl part).[43] The oscillator strengths for both transitions are zero. Thus, direct population of these states upon photoexcitation is prohibited.[68,69] The calculated UV−vis absorption band ($S_0 \rightarrow S_3$) is located at 458 nm. HOMO → LUMO+2 is the major component of the transition.

The electron density is still distributed on the electron-donating group (2,6-diiodoBodipy part), and the transition is not a charge transfer transition. These results are in agreement with the UV−vis absorption experimental results.

The triplet excited states of the compounds were calculated with the TDDFT calculations (see the Supporting Information, Figures S27 and S44, Table S2). For T_1 state, HOMO → LUMO+2 is the main component of the transition. The MOs are localized on the Bodipy unit. The T_2 state is a charge-transfer state for which HOMO → LUMO transition is involved, indicating that the electron is transferred from the electron-donating moiety (2,6-diiodoBodipy part) to the electron-withdrawing moiety (2,4-dinitrobenzenesulfonyl part). Thus, the triplet state of **C-1** will not be quenched by any charge-transfer process. This conclusion is in agreement with the nanosecond transient absorption spectra of **C-1**, indicating that the T_1 state is not completely quenched by PET processes. A similar DFT/TDDFT calculation result was obtained for **C-2** (see Supporting Information, Figure S27 and Table S2).

The fluorescence differences of compounds **1** and **2** were previously studied with the DFT/TDDFT method. The results indicated that the S_1 state of compound **2** is a dark state, due to the electron transfer feature. The S_1 state of compound is an emissive state.[41]

2.6. Jablonski Energy Diagram. The photophysical processes of the compound **C-1** was presented in Scheme 3.

Scheme 3. Simplified Jablonski Diagram Illustrating the Photophysical Processes Involved in (a) C-1 in the Absence of Meracptoethanol and (b) Compound 5 (the Cleaved Product of C-1 in the Presence of Meracptoethanol)[a]

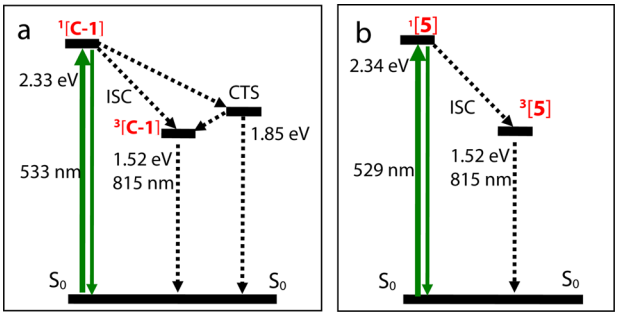

[a]The energy levels of the excited states are designated based on spectral data, electrochemical data, and TDDFT calculations. The number of the superscript designates either the singlet or the triplet excited state. In CH_3CN.

For **C-1**, there is a charge-transfer state (CTS) lying between the singlet state (S_1 state) and the triplet state (T_1 state). TDDFT calculations indicate the CTS is an electron transfer from the iodo-Bodipy unit to the DNBS unit in **C-1** (Figure 8 and Table 4). The energy level of the CTS derived from the electrochemical data is in full agreement with the TDDFT calculations, and it is fully supported by the nanosecond transient absorption spectra (Figure 5).

Thus, the fluorescence of **C-1** may be quenched by the electron transfer. Moreover, the energy gap between the CTS and T_1 states is small; thus, the thermal population of the CTS is possible from the T_1 state. As a result, both mechanisms can quench the triplet state of **C-1**. However, the energy level of the CTS is higher than the T_1 triplet-excited state-energy level; thus, the T_1 state of the Bodipy moiety in **C-1** is not expected to be completely quenched by the PET process. This

DOI: 10.1021/acs.joc.5b00557
J. Org. Chem. 2015, 80, 5674−5686

postulation is in full agreement with the nanosecond transient absorption studies (Figure 5). We studied the singlet oxygen ($^1O_2$) photosensitizing ability of **C-1** in different solvent (see the Supporting Information, Table S1, Figure S29). The result shows that the triplet excited state of **C-1** is unable to be completely quenched in polar solvent such as acetonitrile (Similar results were observed for **C-2**, Supporting Information, Table S1, Figure S28 and S30).

It should be noted that in toluene, the energy level of the CTS state is much higher (2.42 eV, Table 4); thus, neither the fluorescence nor the triplet state of **C-1** is quenched (Figure 4). This theoretical prediction is in agreement with the fluorescence studies. In the presence of thiols, the DNBS moiety was cleaved off the Bodipy moiety. As a result, the CTS is eliminated; thus, the triplet state lifetime of the diiodoBodipy moiety was recovered and the lifetime was extended.[58,59]

2.7. Switching of the Triplet–Triplet Annihilation Upconversion. In recent years, new triplet photosensitizers for TTA upconversion were developed.[38,70−74] TTA upconversion has been also used for luminescence bioimaging[75] and to enhance the photovoltaics.[76,77] However, switching of the TTA upconversion is rarely reported. Herein, the chemical-activated TTA upconversion with **C-1** as triplet photosensitizer was studied (Figure 10 and Table 5). The upconversion

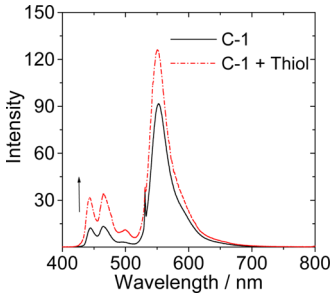

Figure 10. TTA upconversion with **C-1** as triplet photosensitizer, before and after cleavage of the DNBS moiety by mercaptoethanol. Excited with 532 nm CW laser (5 mW, power density: 28 mW cm^{-2}). c[**C-1**] = 1.0 × 10^{-5} M. The optimized perylene concentrations were used c[perylene] = 1.1 × 10^{-4} M for **C-1** and c[perylene] = 9.5 × 10^{-5} M after cleavage of the DNBS moiety by mercaptoethanol. In CH_3CN, 20 °C.

Table 5. Triplet Excited State Lifetimes (τ_T), Stern–Volmer Quenching Constant (K_{sv}), and Bimolecular Quenching Constants (k_q) of the Dyads[a]

	τ_T (μs)	K_{sv} (10^6 M^{-1})	k_q (10^{10} M^{-1} s^{-1})	Φ_{UC}[b] (%)	η[c] (10^3 M^{-1} cm^{-1})
5	171.3	1.6	0.93	5.9	4.8
C-1	24.7	0.2	0.81	0.2	0.1
C-1[d]	86.0	e	e	0.5	0.4

[a]Photosensitizer concentration at 1.0 × 10^{-5} M. In deaerated CH_3CN, 20 °C. [b]Excited with 532 nm laser, with the prompt fluorescence of compound **6** as the standard. [c]Overall upconversion capability, $\eta = \varepsilon \times \Phi_{UC}$, where ε is the molar extinction coefficient of the triplet photosensitizer at the excitation wavelength and Φ_{UC} is the upconversion quantum yield. In M^{-1} cm^{-1}. [d]After cleavage of the DNBS moiety by thiols. (c[**C-1**]:c[thiol] = 1:200). [e]Not determined.

emission was compared with the samples before and after addition of mercaptoethanol. For **C-1** in the absence of thiol, the upconversion fluorescence emission in the range 550–551 nm was observed (with perylene as the triplet acceptor). This result is reasonable because **C-1** shows a triplet excited state (Figure 5). In the presence of thiol, the DNBS moiety of **C-1** was cleaved, the upconversion was intensified (Figure 10), and the upconversion quantum yield increased from 0.2% to 0.5%. The upconversion with compound **5** as triplet photosensitizer was also studied, and the upconversion quantum yield is 5.9% (see Table 5 and the Supporting Information, Figure S31).

TTA upconversion with compounds **1** and **2** as triplet acceptor and PdTPTBP as triplet photosensitizer were studied (Figure 11, Table 6, and the Supporting Information, Figure

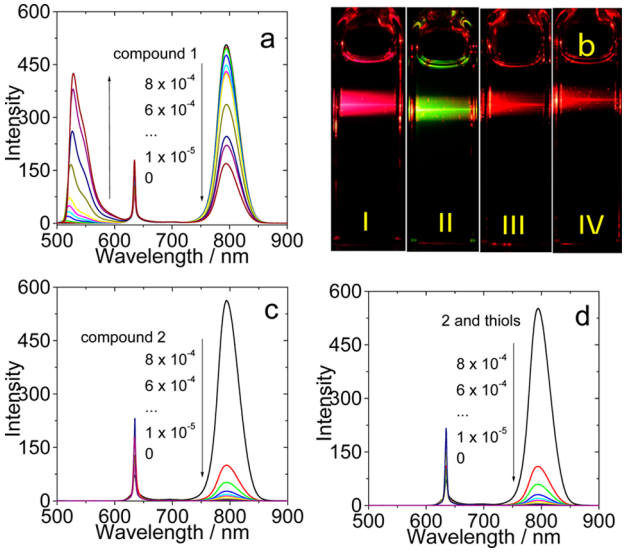

Figure 11. TTA upconversion with PdTPTBP as triplet photosensitizer and compounds **1** or **2** as the triplet acceptor/emitter with (a) increasing amount of compound **1**. (b) Photograph of TTA upconversion (I) without any triplet acceptor, (II) with compound **1** as triplet acceptor;, (III) with compound **2** as triplet acceptor, and (IV) with compound **2** after cleavage of the DNBS moiety by mercaptoethanol as triplet acceptor. Upconversion spectra with (c) **2** as triplet acceptor and (d) **2** upon cleavage by mercaptoethanol. Excited with 635 nm CW laser (5 mW, power density: 28 mW cm^{-2}). c[photosensitizer] = 5.0 × 10^{-6} M in toluene, 20 °C.

S32). With compound **1**, upconversion emission at 528 nm was observed. With compound **2**, however, no upconversion can be observed. Due to the significant quenching effect of the cleavage side product, the switching of the TTA upconversion with compound **2** in the presence of thiol failed (Figure 11d). In order to study the lack of TTA upconversion with compound **2** in the presence of thiol, the quenching of the triplet state of PdTPTBP with compounds **10** and **13** was studied (Figure 14b and the Supporting Information, Figure S40 and S41). The results show that the phosphorescence of PdTPTBP was significantly quenched by compound **10**. Therefore, no upconversion was observed with compound **2** in the presence of mercaptoethanol.

2.8. Mechanism of the Thiol-Switched TTA Upconversion. Quenching of the triplet-state lifetime of the photosensitizer by triplet energy acceptor (perylene) was studied to reveal the origin of different TTA upconversion quantum yields (Figure 12). With perylene as the triplet acceptor (quencher), the quenching constant (K_{SV}) of 1.6 × 10^6 M^{-1} was observed for compound **5** (triplet energy donor), which is much higher than that of **C-1** (K_{SV} = 2.0 × 10^5 M^{-1}). The different quenching constant is due to the different triplet state lifetimes

DOI: 10.1021/acs.joc.5b00557
J. Org. Chem. 2015, 80, 5674−5686

Table 6. Stern–Volmer Quenching Constant (K_{sv}) and Bimolecular Quenching Constants (k_q) of the Triplet Excited State of PdTPTBP Photosensitizers with Compounds 1, 2, 10, and 13 as Quencher[a]

	K_{sv} (10^3 M^{-1})	k_q (M^{-1} s^{-1})	Φ_{UC}[b] (%)	k_0 (10^{10} M^{-1} s^{-1})/f_Q (%)	η[c] (10^3 M^{-1} cm^{-1})
1	5.7×10^3	3.1×10^7	21.5	1.16/0.3	5.0
2	6.9×10^5	4.0×10^9	*d*	1.11/36.4	*d*
10	7.2×10^3	4.3×10^7	*d*	1.23/0.4	*d*
13	9.3×10^5	5.1×10^9	*d*	1.14/44.6	*d*

[a]All the data were obtained with photosensitizer concentration at 5.0 × 10^{-6} M. In deaerated toluene, 20 °C. [b]Excited with 635 nm laser, with the prompt phosphorescence quantum yields (16.7%) of PdTPTBP as the standard. [c]Overall upconversion capability, $\eta = \varepsilon \times \Phi_{UC}$, where ε is the molar extinction coefficient of the triplet photosensitizer at the excitation wavelength and Φ_{UC} is the upconversion quantum yield. [d]Not applicable.

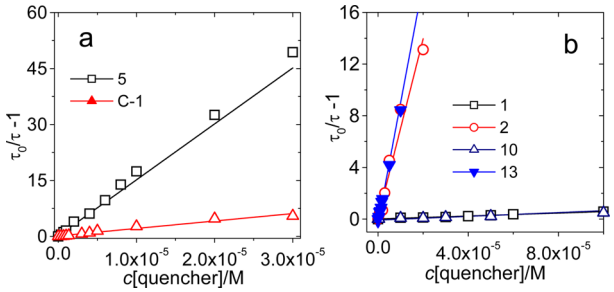

Figure 12. Stern–Volmer plots for quenching of the triplet lifetime of photosensitizers with triplet energy acceptor. (a) Perylene as the triplet acceptor, **5** and **C-1** as triplet photosensitizers. *c*[photosensitizers] = 1.0 × 10^{-5} M. In CH_3CN. (b) Compounds **1**, **2**, **10**, and **13** as the triplet acceptor, PdTPTBP as photosensitizers. The triplet excited-state lifetimes were measured with transient absorption spectrum. *c*[photosensitizers] = 5.0 × 10^{-6} M in toluene, 20 °C.

of compound **5** (τ_T = 171.3 μs) and **C-1** (τ_T = 24.7 μs).[51] A longer triplet-state lifetime is beneficial for the TTET process; thus, a higher TTA upconversion quantum yield was observed with compound **5** (Φ_{UC} = 5.9%) than that of **C-1** (Φ_{UC} = 0.2%) (for more details, see Figure 12, Table 5, and the Supporting Information, Figures S36 and S37).

The quenching efficiency was studied (eq 6), where k_0 is the diffusion-controlled bimolecular quenching rating constant and can be calculated with the Smoluchowski equation (eq 7).[51]

$$f_Q = k_q/k_0 \tag{6}$$

$$k_0 = 4\pi RND/1000 = \frac{4\pi N}{1000}(R_f + R_q)(D_f + D_q) \tag{7}$$

Here, D is the sum of the diffusion coefficients of the energy donor (D_f) and quencher (D_q), and N is Avogadro's number. R is the collision radius, the sum of the molecule radii of the energy donor (R_f) and the quencher (R_q). Diffusion coefficients can be obtained from Stokes–Einstein equation (eq 8)[51]

$$D = kT/6\pi\eta R \tag{8}$$

where k is Boltzmann's constant, η is the solvent viscosity, and R is the molecule radius. The molecule radius of the energy donor (compound **5**) is 5.7 and 4.8 Å for the quencher (perylene). According to eq 8, the diffusion coefficients of the energy donor (**5**) are 9.87 × 10^{-6} and 1.17 × 10^{-6} cm^2 s^{-1} for quencher (perylene) (in acetonitrile at 15 °C). Thus, k_0 was calculated as 1.72 × 10^{10} M^{-1} s^{-1}. Since k_q = 9.3 × 10^9 M^{-1} s^{-1} (Table 4), the quenching efficiency was calculated as 54.4% according to eq 9, indicating that there is an efficient triplet-state energy transfer between compound **5** and perylene.

On the basis of the optimized ground-state geometry of the compounds, the molecule radii of the energy donor (**C-1**) is 5.1 Å and that of quencher (perylene) is 4.8 Å. According to eq 11, the diffusion coefficient of the energy donor (**C-1**) is 1.10 × 10^{-6} cm^2 s^{-1} and that of quencher (perylene) is 1.17 × 10^{-6} cm^2 s^{-1} (in acetonitrile at 15 °C). Thus, k_0 was calculated as 1.71 × 10^{10} M^{-1} s^{-1}. The quenching efficiency was calculated as 47.4% according to eq 6, indicating that there is moderate triplet-state energy transfer between **C-1** and perylene in the mixture.

2.9. Conclusions. In summary, the *different* quenching effects of an electron acceptor on the singlet and triplet excited states of Bodipy chromophore were studied. The triplet-state formation or fluorescence of Bodipy was caged with 2,4-dinitrobenzenenesulfonyl (DNBS), which can be cleaved by thiols, such as mercaptoethanol. The photophysical properties of the compounds were studied with steady-state UV–vis absorption spectroscopy, fluorescence spectroscopy, electrochemical characterization, Gibbs free energy changes, nanosecond transient absorption spectroscopy, and DFT/TDDFT computations. The DNBS-caged triplet photosensitizer shows a shorter triplet-state lifetime (τ_T = 24.7 μs, singlet oxygen quantum yield Φ_Δ = 74%) than the uncaged diiodoBodipy triplet photosensitizer (τ_T = 86.0 μs, Φ_Δ = 88%). On the other hand, the DNBS-caged fluorophore shows very weak fluorescence emission (fluorescence quantum yield Φ_F = 0.6%), but the uncaged fluorophore shows enhanced fluorescence (Φ_F = 50.0%). These studies indicate that the DNBS moiety exerts different quenching effects on the singlet excited state and triplet excited state of the same chromophore. The quenching effect of the DNBS moiety on the singlet excited state of Bodipy is more efficient than the quenching of the triplet excited state. The reason was revealed with calculation of the Gibbs free energy changes of the electron transfer in that the singlet state, with a higher energy level than the triplet excited state, produces a larger driving force for the PET process than the triplet excited state. As a proof of concept, the thiol-activated triplet–triplet annihilation (TTA) upconversion was studied with DNBS-caged diiodoBodipy triplet photosensitizers (with perylene as the triplet acceptor/emitter of the upconversion) or DNBS-caged Bodipy fluorophore (as triplet acceptor/emitter, with PdTPTBP as the triplet photosensitizer). This information may be useful for designing efficient external stimuli-activatable triplet photosensitizers and for application of these compounds in stimuli-activatable photodynamic therapy, controllable TTA upconversion, as well as molecular logic gates.

3. EXPERIMENTAL SECTION

3.1. General Methods. In cyclic voltammogram measurements, ferrocene (Fc) was used as internal reference ($E_1/_2$ = +0.64 V (Fc^+/Fc) vs standard hydrogen electrode). All of the samples in cyclic voltammogram experiments were deaerated with Ar for 15 min before

DOI: 10.1021/acs.joc.5b00557
J. Org. Chem. 2015, 80, 5674–5686

measurement. In deaerated CH_3CN solutions containing 1.0 mM photosensitizers, or with the ferrocene, 0.10 M Bu_4NPF_6 as supporting electrolyte, $Ag/AgNO_3$ reference electrode, scan rates 0.1 V/s. The compounds **1**−**13** were prepared following the reported methods.[52] The ^1H NMR data were correct by TMS and ^{13}C NMR data were correct by the solvent residual peaks (TMS, etc.).[78]

3.2. Synthesis of Compound 2.[41] Compound **1** (100 mg, 0.3 mmol) was added into dry CH_2Cl_2 (10 mL at 25 °C). Then triethylamine (0.1 mmol) was added. The reaction mixture was vigorously stirred for 5 min. After that, a solution of 2,4-dinitrobenzenesulfonyl chloride (235.0 mg, 0.9 mmol) in CH_2Cl_2 was added dropwise at 0 °C. The reaction mixture was stirred for 2 h at 50 °C. Then the solvent was removed under reduced pressure, and the crude product was subjected to column chromatography (silica gel, DCM/petroleum ether, 1:2, v/v). Compound **2** was obtained as an orange-red solid (102 mg, 59.7%): mp 190.0−192.0 °C; ^1H NMR (400 MHz, $CDCl_3$) δ 8.69 (s, 1H), 8.50 (d, 1H, J = 8.8 Hz), 8.21 (d, 1H, J = 8.8 Hz), 7.41 (d, 2H, J = 8.4 Hz), 7.36 (d, 2H, J = 8.4 Hz), 6.00 (s, 2H), 2.55 (s, 6H), 1.33 (s, 6H); MALDI−HRMS (TOF) calcd ($[C_{25}H_{21}BN_4O_7F_2S]^+$) m/z = 570.1192, found m/z = 570.1184.

3.3. Synthesis of Compound C-1. Compound **2** (285 mg, 0.5 mmol) and *N*-iodosuccinimide (NIS) (450 mg, 2 mmol) were added into dry CH_2Cl_2 (50 mL). Under N_2 atmosphere, the solution was stirred for 5 h. The solvent was removed under reduced pressure. The crude product was purified by column chromatography (silica gel; CH_2Cl_2/petroleum ether, 1/2, v/v): yield 288 mg (70%); mp > 250 °C; ^1H NMR (500 MHz, $CDCl_3$) δ 8.71 (d, 1H, J = 2.0 Hz), 8.57−8.54 (m, 1H), 8.27 (d, 1H, J = 13.0 Hz), 7.44 (d, 2H, J = 8.5 Hz), 7.34 (d, 2H, J = 8.5 Hz), 2.65 (s, 6H,), 1.36 (s, 6H); ^{13}C NMR (100 MHz, DMSO-d_6) δ 156.4, 151.6, 149.3, 148.2, 144.7, 139.7, 133.9, 130.6, 130.4, 130.0, 127.3, 123.3, 121.1, 87.2, 16.8, 15.8; MALDI−HRMS (TOF) calcd ($[C_{25}H_{19}BN_4O_7F_2SI_2]^+$) m/z = 821.9125, found m/z = 821.9139.

3.4. Synthesis of Compound 4.[52] Synthesis method was similar to compound **C-1**: yield 263 mg (73%); mp > 250 °C. ^1H NMR (400 MHz, $CDCl_3$) δ 7.94 (d, 2H, J = 7.6 Hz), 7.27 (s, 1H), 7.25 (s, 1H), 2.64 (s, 6H), 1.40 (s, 12H), 1.37 (s, 6H); ^{13}C NMR (100 MHz, $CDCl_3$) δ 157.0, 145.6, 141.4, 137.6, 135.8, 131.2, 127.3, 85.8, 84.4, 25.1, 17.3, 16.2; MALDI−HRMS (TOF) calcd ($[C_{25}H_{28}B_2N_2O_2F_2I_2]^+$) m/z = 702.0394, found m/z = 702.0372.

3.5. Synthesis of Compound 5.[79] A mixture of compound **4** (702 mg, 1 mmol), 30% H_2O_2 (0.5 mL), water (2.0 mL), and urea (7.6 mg, 0.1 mmol) was stirred at room temperature (rt). After completion of the reaction (indicated by TLC), the reaction mixture was extracted with DCM. The organic layer was dried with anhydrous sodium sulfate. The solvent was removed under reduced pressure. The crude product was purified by column chromatography (silica gel, petroleum ether/DCM = 1:1, v/v): yield 301 mg (43.0%); mp > 250 °C; ^1H NMR (500 MHz, DMSO-d_6) δ 9.95 (s, 1H), 7.16 (d, 2H, J = 8.5 Hz), 6.95 (d, 2H, J = 8.5 Hz), 2.53 (s, 6H), 1.43 (s, 6H); ^{13}C NMR (125 MHz, DMSO-d_6) δ 158.6, 155.6, 145.0, 142.7, 131.3, 129.1, 124.0, 116.3, 86.6, 16.7, 15.7; MALDI−HRMS (TOF) calcd ($[C_{19}H_{17}BN_2OF_2I_2]^+$) m/z = 591.9491, found m/z = 591.9499.

3.6. Synthesis of Compound 7. Under N_2 atmosphere, a mixture of **6** (576 mg, 1 mmol), *p*-hydroxybenzaldehyde (122 mg, 1 mmol), piperidine (three drops), and acetic acid (three drops) was dissolved in dry toluene (100 mL). The reaction solution was reflux at 120 °C for 10 min, and then the reaction solution was cooled to rt and the reaction was quenched by water. The solution was extracted with CH_2Cl_2. The organic layers were dried with Na_2SO_4. The organic solution was concentrated under reduced pressure. The crude product was further purified using column chromatography (silica gel, CH_2Cl_2) to give **7** as a dark blue power: yield 82 mg (12%); mp > 250 °C; ^1H NMR (400 MHz, $CDCl_3$) δ 8.12 (d, 1H, J = 16.8 Hz), 7.56−7.51 (m, 6H), 7.28−7.27 (t, 2H, J = 5.6 Hz), 6.87 (d, 2H, J = 8.8 Hz), 2.69 (s, 3H), 1.44 (s, 3H), 1.39 (s, 3H); ^{13}C NMR (100 MHz, DMSO-d_6) δ 159.4, 155.7, 150.1, 145.9, 144.3, 140.2, 139.0, 134.1, 131.8, 131.3, 129.5, 129.0, 128.0, 127.0, 116.2, 114.9, 87.3, 83.6, 17.0, 16.5, 15.9; MALDI−HRMS (TOF) calcd for ($[C_{26}H_{21}BN_2OF_2I_2]^+$) m/z = 679.9804, found m/z = 679.9824.

3.7. Synthesis of Compound C-2.[41] Compound 7 (34 mg, 0.05 mmol) was added into dry CH_2Cl_2 (10 mL at 25 °C). Then triethylamine (0.1 mmol) was added into the solution. The reaction solution was vigorously stirred for 5 min. After that, a solution of 2,4-dinitrobenzenesulfonyl chloride (40.0 mg, 0.15 mmol) in CH_2Cl_2 was added dropwise at 0 °C. The reaction solution was stirred for 2 h at 50 °C. The solvent was removed under reduced pressure, and the crude product was subjected to column chromatography (silica gel, DCM/petroleum ether, 1:1, v/v). **C-2** was obtained as a dark-blue solid (26 mg, 57%): mp > 250.0 °C; ^1H NMR (500 MHz, DMSO-d_6) δ 9.13 (d, 1H, J = 2.5 Hz), 8.62−8.60 (m, 1H), 8.28 (d, 1H, J = 8.5 Hz), 7.98 (d, 1H, J = 16.5 Hz), 7.68 (s, 1H), 7.66 (s, 1H), 7.62−7.60 (m, 3H), 7.45−7.43 (m, 3H), 7.30 (d, 2H, J = 9.0 Hz), 2.59 (s, 3H), 1.39 (s, 3H), 1.36 (s, 3H); no satisfactory ^{13}C NMR data were obtained due to the poor solubility of the compound; MALDI−HRMS (TOF) calcd for ($[C_{32}H_{23}BN_4O_7F_2SI_2]^+$) m/z = 909.9438, found m/z = 909.9445.

3.8. Synthesis of Compound 10.[80] Mercaptoethanol (5.2 mmol) in 20 mL of dry $CHCl_3$ was slowly added to a solution of 2,4-dinitrofluorobenzene (1 g, 5.2 mmol) in triethylamine (7 mL) at room temperature. The reaction process was monitored by TLC. The mixture was extracted with HCl (1 M), and then the organic layer was washed twice with water. The product was separated, dried over magnesium sulfate ($MgSO_4$), filtered, and concentrated under vacuum. Crude products were then recrystallized from $CHCl_3$, giving a bright yellow solid: yield 783 mg (65%); mp 100.0−100.5 °C; ^1H NMR (500 MHz, $CDCl_3$) δ 9.08 (d, 1 H, J = 2.5 Hz), 8.39−8.36 (m, 1H), 7.69 (d, 1H, J = 9.0 Hz), 4.05 (t, 2H, J = 12.0 Hz), 3.32 (t, 2H, J = 12.0 Hz); TOF HR MS EI$^+$ calcd for ($[C_8H_8N_2O_5S]^+$) m/z = 244.0154, found m/z = 244.0163.

3.9. Synthesis of Compound 13.[41] The synthesis method was similar to that used for compound **2**: yield 146 mg (54%); mp 112.8−113.5 °C; ^1H NMR (500 MHz, $CDCl_3$) δ 8.65 (d, 1 H, J = 2.5 Hz), 8.49−8.46 (m, 1H), 8.19 (d, 1H, J = 9.0 Hz), 7.40−7.34 (m, 3H), 7.22−7.20 (m, 2H); TOF HR MS EI$^+$ calcd for ($[C_{12}H_8N_2O_7S]^+$) m/z = 324.0052, found m/z = 324.0060

3.10. Cyclic Voltammetry. Cyclic voltammetry was performed using a CHI610D electrochemical workstation (Shanghai, China). Cyclic voltammograms were recorded at scan rates of 0.1 V/s. The electrolytic cell used was a three-electrode cell. Electrochemical measurements were performed at 20 °C using 0.1 M tetrabutylammonium hexafluorophosphate ($Bu_4N[PF_6]$) as supporting electrolyte. All of the samples were deaerated with N_2 for 15 min before measurement. The working electrode was a glassy carbon electrode, and the counter electrode was a platinum electrode. A nonaqueous $Ag/AgNO_3$ (0.1 M in acetonitrile) reference electrode was contained in a separate compartment connected to the solution via semipermeable membrane. DCM was used as the solvent. Ferrocene was added as the internal references.

3.11. Nanosecond Transient Absorption Spectra. The nanosecond transient absorption spectra were measured on a LP920 laser flash photolysis spectrometer, and the signal was digitized with an oscilloscope. The lifetime values of triplet-state photosensitizers were obtained by monitoring the decay trace of the transients with the LP900 software. All samples in flash photolysis experiments were deaerated with N_2 for ca. 15 min before measurement, and the gas flow was maintained during the measurement.

3.12. Triplet State Quantum Yield.[81] Triplet state quantum yield (Φ_T) was measured based on the singlet-state depletion method using LP920 ns transient absorption laser flash photolysis spectrometer. Triplet-state quantum yield were calculated with Rose Bengal (RB) as standard (Φ_T = 0.9 in methanol). Optically matched solutions of RB and the photosensitizers were used (A = 0.13 at 537 nm). The sample solution was degassed for at least 15 min with N_2 or Ar, and the gas flow was kept during the measurement. Triplet-state quantum yields (Φ_T) were calculated according to the following equation (eq 9)

$$\Phi_T^{bod} = \Phi_T^{ref} \times \frac{\varepsilon^{ref}}{\varepsilon_{bod}} \times \frac{\Delta A_s^{bod}}{\Delta A_s^{ref}} \quad (9)$$

DOI: 10.1021/acs.joc.5b00557
J. Org. Chem. 2015, 80, 5674−5686

where ϵ is the molar absorption coefficient of the compounds at the ground state and ΔA is the optical density value at the bleaching band maximum. The superscript "bod" indicates the sample, and "ref" indicates the reference compound (Rose Bengal).

■ ASSOCIATED CONTENT

Supporting Information

Molecular structure characterization, transient absorption spectra, additional UV−vis absorption, and fluorescence spectra and the optimized geometries. The Supporting Information is available free of charge on the ACS Publications website at DOI: 10.1021/acs.joc.5b00557.

■ AUTHOR INFORMATION

Corresponding Author

*E-mail: zhaojzh@dlut.edu.cn.

Notes

The authors declare no competing financial interest.

■ ACKNOWLEDGMENTS

We thank the NSFC (21073028, 21273028, 21473020, and 21421005), the Royal Society (UK) and NSFC (China-UK Cost-Share Science Networks, 21011130154), the Ministry of Education (SRFDP-20120041130005), the Fundamental Research Funds for the Central Universities (DUT14ZD226), the Program for Changjiang Scholars and Innovative Research Team in University [IRT_132206], and Dalian University of Technology for financial support (DUT2013TB07).

■ REFERENCES

(1) de Silva, A. P.; Gunaratne, H. Q. N.; Gunnlaugsson, T.; Huxley, A. J. M.; McCoy, C. P.; Rademacher, J. T.; Rice, T. E. *Chem. Rev.* **1997**, *97*, 1515−1566.
(2) Chen, X.; Zhou, Y.; Peng, X.; Yoon, J. *Chem. Soc. Rev.* **2010**, *39*, 2120−2135.
(3) Guo, Z.; Zhu, W.; Tian, H. *Chem. Commun.* **2012**, *48*, 6073−6084.
(4) Wu, Y.; Xie, Y.; Zhang, Q.; Tian, H.; Zhu, W.; Li, A. D. Q. *Angew. Chem., Int. Ed.* **2014**, *53*, 2090−2094.
(5) Kand, D.; Mandal, P. S.; Sahaa, T.; Talukdar, P. *RSC Adv.* **2014**, *4*, 59579−59586.
(6) Roy, A.; Kand, D.; Saha, T.; Talukdar, P. *Chem. Commun.* **2014**, *50*, 5510−5513.
(7) Huang, Z.; Yu, S.; Wen, K.; Yu, X.; Pu, L. *Chem. Sci.* **2014**, *5*, 3457−3462.
(8) Panizzi, P.; Nahrendorf, M.; Wildgruber, M.; Waterman, P.; Figueiredo, J.; Aikawa, E.; McCarthy, J.; Weissleder, R.; Hilderbrand, S. A. *J. Am. Chem. Soc.* **2009**, *131*, 15739−15744.
(9) Huang, Z.; Yu, S.; Zhao, X.; Wen, K.; Xu, Y.; Yu, X.; Xu, Y.; Pu, L. *Chem.—Eur. J.* **2014**, *20*, 16458−16461.
(10) Golovkova, T. A.; Kozlov, D. V.; Neckers, D. C. *J. Org. Chem.* **2005**, *70*, 5545−5549.
(11) Pu, S.; Tong, Z.; Liu, G.; Wang, R. *J. Mater. Chem. C* **2013**, *1*, 4726−4739.
(12) Erbas−Cakmak, S.; Akkaya, E. U. *Angew. Chem., Int. Ed.* **2013**, *52*, 11364−11368.
(13) Harriman, A.; Mallon, L. J.; Elliot, K. J.; Haefele, A.; Ulrich, G.; Ziessel, R. *J. Am. Chem. Soc.* **2009**, *131*, 13375−13386.
(14) Erbas-Cakmak, S.; Bozdemir, O. A.; Cakmaka, Y.; Akkaya, E. U. *Chem. Sci.* **2013**, *4*, 858−862.
(15) Areephong, J.; Browne, W. R.; Feringa, B. L. *Org. Biomed. Chem.* **2007**, *5*, 1170−1174.
(16) Bai, D.; Benniston, A. C.; Hagon, J.; Lemmetyinen, H.; Tkachenko, N. V.; Harringtonc, R. W. *Phys. Chem. Chem. Phys.* **2013**, *15*, 9854−9861.
(17) Shi, W.; Menting, R.; Ermilov, E. A.; Lo, P.; Röderb, B.; Ng, D. K. P. *Chem. Commun.* **2013**, *49*, 5277−5279.
(18) Wu, W.; Kirillov, A. M.; Yan, X.; Zhou, P.; Liu, W.; Tang, Y. *Angew. Chem., Int. Ed.* **2014**, *53*, 10649−10653.
(19) Jukes, R. T. F.; Adamo, V.; Hartl, F.; Belser, P.; Cola, L. D. *Inorg. Chem.* **2004**, *43*, 2779−2792.
(20) McDonnell, S. O.; Hall, M. J.; Allen, L. T.; Byrne, A.; Gallagher, W. M.; O'Shea, D. F. *J. Am. Chem. Soc.* **2005**, *127*, 16360−16361.
(21) Indelli, M. T.; Carli, S.; Ghirotti, M.; Chiorboli, C.; Ravaglia, M.; Garavelli, M.; Scandola, F. *J. Am. Chem. Soc.* **2008**, *130*, 7286−7299.
(22) Chan, J. C.; Lam, W. H.; Wong, H.; Zhu, N.; Wong, W.; Yam, V. W. *J. Am. Chem. Soc.* **2011**, *133*, 12690−12705.
(23) Stefflova, K.; Li, H.; Chen, J.; Zheng, G. *Bioconjugate Chem.* **2007**, *18*, 379−388.
(24) Tian, J.; Ding, L.; Xu, H.; Shen, Z.; Ju, H.; Jia, L.; Bao, L.; Yu, J. *J. Am. Chem. Soc.* **2013**, *135*, 18850−18858.
(25) Lau, J. T. F.; Jiang, X.; Ng, D. K. P.; Lo, P. *Chem. Commun.* **2013**, *49*, 4274−4276.
(26) Lau, J. T. F.; Lo, P.; Jiang, X.; Wang, Q.; Ng, D. K. P. *J. Med. Chem.* **2014**, *57*, 4088−4097.
(27) Jiang, X.; Lo, P.; Tsang, Y.; Yeung, S.; Fong, W.; Ng, D. K. P. *Chem.—Eur. J.* **2010**, *16*, 4777−4783.
(28) Irie, M. *Chem. Rev.* **2000**, *100*, 1685−1716.
(29) Hou, L.; Zhang, X.; Pijper, T. C.; Browne, W. R.; Feringa, B. L. *J. Am. Chem. Soc.* **2014**, *136*, 910−913.
(30) Ji, S.; Guo, H.; Yuan, X.; Li, X.; Ding, H.; Gao, P.; Zhao, C.; Wu, W.; Wu, W.; Zhao, J. *Org. Lett.* **2010**, *12*, 2876−2879.
(31) He, H.; Lo, P.; Ng, D. K. P. *Chem.—Eur. J.* **2014**, *20*, 6241−6245.
(32) Turan, I. S.; Cakmak, F. P.; Yildirim, D. C.; Cetin-Atalay, R.; Akkaya, E. U. *Chem.—Eur. J.* **2014**, *20*, 16088−16092.
(33) Ma, J.; Cui, X.; Wang, F.; Wu, X.; Zhao, J.; Li, X. *J. Org. Chem.* **2014**, *79*, 10855−10866.
(34) Cui, X.; Zhao, J.; Zhou, Y.; Ma, J.; Zhao, Y. *J. Am. Chem. Soc.* **2014**, *136*, 9256−9259.
(35) Ozlem, S.; Akkaya, E. U. *J. Am. Chem. Soc.* **2009**, *131*, 48−49.
(36) Wang, F.; Cui, X.; Lou, Z.; Zhao, J.; Bao, M.; Li, X. *Chem. Commun.* **2014**, *50*, 15627−15630.
(37) Ji, S.; Wu, W.; Wu, W.; Guo, H.; Zhao, J. *Angew. Chem., Int. Ed.* **2011**, *50*, 1626−1629.
(38) Peng, J.; Jiang, X.; Guo, X.; Zhao, D.; Ma, Y. *Chem. Commun.* **2014**, *50*, 7828−7830.
(39) Jiang, W.; Fu, Q.; Fan, H.; Ho, J.; Wang, W. *Angew. Chem., Int. Ed.* **2007**, *46*, 8445−8448.
(40) Ji, S.; Yang, J.; Yang, Q.; Liu, S.; Chen, M.; Zhao, J. *J. Org. Chem.* **2009**, *74*, 4855−4865.
(41) Guo, H.; Jing, Y.; Yuan, X.; Ji, S.; Zhao, J.; Lib, X.; Kanc, Y. *Org. Biomol. Chem.* **2011**, *9*, 3844−3853.
(42) Li, X.; Qian, S.; He, Q.; Yang, B.; Li, J.; Hu, Y. *Org. Biomol. Chem.* **2010**, *8*, 3627−3630.
(43) Bouffard, J.; Kim, Y.; Swager, T. M.; Weissleder, R.; Hilderbrand, S. A. *Org. Lett.* **2008**, *1*, 37−40.
(44) Wang, S.; Deng, W.; Sun, D.; Yan, M.; Zheng, H.; Xu, J. *Org. Biomol. Chem.* **2009**, *7*, 4017−4020.
(45) Ulrich, G.; Ziessel, R.; Harriman, A. *Angew. Chem., Int. Ed.* **2008**, *47*, 1184−1201.
(46) Benniston, A. C.; Copley, G. *Phys. Chem. Chem. Phys.* **2009**, *11*, 4124−4131.
(47) Loudet, A.; Burgess, K. *Chem. Rev.* **2007**, *107*, 4891−4932.
(48) Lu, H.; Mack, J.; Yang, Y.; Shen, Z. *Chem. Soc. Rev.* **2014**, *43*, 4778−4823.
(49) Chen, Y.; Qi, D.; Zhao, L.; Cao, W.; Huang, C.; Jiang, J. *Chem.—Eur. J.* **2013**, *19*, 7342−7347.
(50) Alamiry, M. A. H.; Benniston, A. C.; Copley, G.; Harriman, A.; Howgego, D. *J. Phys. Chem. A* **2011**, *115*, 12111−12119.
(51) Lakowicz, J. R. *Principles of Fluorescence Spectroscopy*, 2nd ed.; Kluwer Academic: New York, 1999.
(52) Wu, W.; Guo, H.; Wu, W.; Ji, S.; Zhao, J. *J. Org. Chem.* **2011**, *76*, 7056−7064.

DOI: 10.1021/acs.joc.5b00557
J. Org. Chem. 2015, 80, 5674−5686

(53) Kamkaew, A.; Lim, S. H.; Lee, H. B.; Kiew, L. V.; Chung, L. Y.; Burgess, K. *Chem. Soc. Rev.* **2013**, *42*, 77−88.
(54) Awuahab, S. G.; You, Y. *RSC Adv.* **2012**, *2*, 11169−11183.
(55) Yogo, T.; Urano, Y.; Ishitsuka, Y.; Maniwa, F.; Nagano, T. *J. Am. Chem. Soc.* **2005**, *127*, 12162−12163.
(56) Apperloo, J. J.; Martineau, C.; Hal, P. A. V.; Roncali, J.; Janssen, R. A. J. *Asian J. Phys. Chem. A* **2002**, *106*, 21−31.
(57) Sabatini, R. P.; McCormick, T. M.; Lazarides, T.; Wilson, K. C.; Eisenberg, R.; McCamant, D. W. *J. Phys. Chem. Lett.* **2011**, *2*, 223−227.
(58) El-Khouly, M. E.; Amin, A. N.; Zandler, M. E.; Fukuzumi, S.; Souza, F. D. *Chem.—Eur. J.* **2012**, *18*, 5239−5247.
(59) Ziessel, R.; Allen, B. D.; Rewinska, D. B.; Harriman, A. *Chem.—Eur. J.* **2009**, *15*, 7382−7393.
(60) Hofmann, C. C.; Lindner, S. M.; Ruppert, M.; Hirsch, A.; Haque, S. A.; Thelakkat, M.; Köhler, J. *J. Phys. Chem. B* **2010**, *114*, 9148−9156.
(61) El-Khouly, M. E.; Fukuzumi, S. *J. Porphyrins Phthalocyanines* **2011**, *15*, 111−117.
(62) Adamoab, C.; Jacquemin, D. *Chem. Soc. Rev.* **2013**, *42*, 845−856.
(63) Wang, D.; Guo, J.; Ren, A.; Huang, S.; Zhang, L.; Feng, J. *J. Phys. Chem. B* **2014**, *118*, 10101−10110.
(64) Zou, L.; Ren, A.; Feng, J.; Liu, Y.; Ran, X.; Sun, C. *J. Phys. Chem. A* **2008**, *112*, 12172−12178.
(65) Wu, J.; Kan, Y.; Wu, Y.; Su, Z. *J. Phys. Chem. C* **2013**, *117*, 8420−8428.
(66) Steffen, A.; Costuas, K.; Boucekkine, A.; Thibault, M.-H.; Beeby, A.; Batsanov, A. S.; Charaf-Eddin, A.; Jacquemin, D.; Halet, J.-F.; Marder, T. B. *Inorg. Chem.* **2014**, *53*, 7055−7069.
(67) Hanson, K.; Tamayo, A.; Diev, V. V.; Whited, M. T.; Djurovich, P. I.; Thompson, M. E. *Inorg. Chem.* **2010**, *49*, 6077−6084.
(68) Turro, N. J.; Ramamurthy, V.; Scaiano, J. C. *Principles of Molecular Photochemistry: An Introduction*; University Science Books: Sausalito, CA, 2009.
(69) Zhao, G.-J.; Liu, J.-Y.; Zhou, L.-C.; Han, K.-L. *J. Phys. Chem. B* **2007**, *111*, 8940−8945.
(70) (a) Singh-Rachford, T. N.; Castellano, F. N. *Coord. Chem. Rev.* **2010**, *254*, 2560−2573. (b) Zhou, J.; Liu, Q.; Feng, W.; Sun, Y.; Li, F. *Chem. Rev.* **2015**, *115*, 395−465.
(71) Ceroni, P. *Chem.—Eur. J.* **2011**, *17*, 9560−9564.
(72) Zhao, J.; Wu, W.; Sun, J.; Guo, S. *Chem. Soc. Rev.* **2013**, *42*, 5323−5351.
(73) Monguzzi, A.; Tubino, R.; Hoseinkhani, S.; Campioneb, M.; Meinardib, F. *Phys. Chem. Chem. Phys.* **2012**, *14*, 4322−4332.
(74) (a) Simon, Y. C.; Weder, C. *J. Mater. Chem.* **2012**, *22*, 20817−20830. (b) Cao, X.; Hu, B.; Zhang, P. *J. Phys. Chem. Lett.* **2013**, *4*, 2334−2338.
(75) Liu, Q.; Yang, T.; Feng, W.; Li, F. J. *Am. Chem. Soc.* **2012**, *134*, 5390−5397.
(76) Lissau, J. S.; Gardner, J. M.; Morandeira, A. *J. Phys. Chem. C* **2011**, *115*, 23226−23232.
(77) Cheng, Y. Y.; Fückel, B.; MacQueen, R. W.; Khoury, T.; Clady, R. G. C. R.; Schulze, T. F.; Ekins-Daukes, N. J.; Crossley, M. J.; Stannowski, B.; Lips, K.; Schmidtxae, T. W. *Energy Environ. Sci.* **2012**, *5*, 6953−6959.
(78) Gottlieb, H. E.; Kotlyar, V.; Nudelman, A. *J. Org. Chem.* **1997**, *62*, 7512−7515.
(79) Wang, L.; Dai, D.; Chen, Q.; He, M. *Asian J. Org. Chem.* **2013**, *2*, 1040−1043.
(80) Carrot, G.; Hilborn, J. G.; Trollsås, M.; Hedrick, J. L. *Macromolecules* **1999**, *32*, 5264−5269.
(81) (a) Li, Y.; Dandu, N.; Liu, R.; Li, Z.; Kilina, S.; Sun, W. *J. Phys. Chem. C* **2014**, *118*, 6372−6384. (b) Rondão, R.; de Melo, J. S. S. *J. Phys. Chem. C* **2013**, *117*, 603−614.

DOI: 10.1021/acs.joc.5b00557
J. Org. Chem. 2015, 80, 5674−5686